Distributed Active Filter Systems (DAFS): A new approach to power system harmonics

Po-Tai Cheng Zhung-Lin Lee
CENTER FOR ADVANCED POWER TECHNOLOGIES (CAPT)
Department of Electrical Engineering
National Tsing Hua University
Hsin-Chu, 30013, TAIWAN
email: ptcheng@ee.nthu.edu.tw; d907904@oz.nthu.edu.tw

***Abstract*— This paper proposes a distributed active filter system (DAFS) for alleviating the harmonic distortion of power systems. The proposed DAFS consists of multiple active filter units installed on the same location or different locations within the power system. The active filter units of the proposed DAFS can cooperate, without any communication among them, to reduce the voltage harmonic distortion of the power lines. Each individual active filter unit functions like a harmonic conductance to reduce voltage harmonics. A droop relationship between the harmonic conductance and the volt-ampere of the active filter unit is programmed into the controller of each unit so multiple active filter units can share the workload of harmonic filtering. The slope of the droop is determined by the volt-ampere rating of the active filter unit in order to distribute the harmonic filtering workload in proportion to the rated capacity of each unit. The principle of operation is explained in this paper and test results based on computer simulation and laboratory test bench are provided to validate the functionalities of the proposed DAFS.**

I. INTRODUCTION

The proliferation of nonlinear loads in the power system has been growing in an unprecedented pace in recent years due to the advance of power electronics technologies. As a result, the harmonic pollution in the power system deteriorates significantly. Harmonic resonance which results in severe voltage distortion has been reported. Previous literatures proposes installation of active filter at the end of radial lines to damp the harmonic resonance[1], [2]. However, depending on the magnitude of damping provided by the active filter, the level of harmonic distortion may become worse at certain locations along the radial line. Multiple installations of active filters have been presented in [2], but real-time communications among various units are required to coordinate the operations.

A distributed active filter system (DAFS) is proposed in this paper to reduce voltage harmonic distortion of power systems. The proposed DAFS consists of several active filter units installed on various locations, and each unit operates as a harmonic conductance to reduce the voltage harmonics. The active filter units of the DAFS can share the harmonic filtering workload without any communications among them. This feature is accomplished by the droop relationship between the harmonic conductance and the volt-ampere of each active filter. The slope of the droop programmed into each active filter is determined by the volt-ampere rating of the active filter to ensure that the sharing of filtering workload is in proportion to the capacity of the active filter. Using the droop characteristic to share the current of a certain harmonic frequency has been presented in [3]. The proposed DAFS can share the harmonics within the operation bandwidth of the active filter units.

II. PRINCIPLES OF OPERATION

A simplified one-line diagram of the proposed DAFS is shown in figure 1. Several active filter units, including AFU_x, AFU_y, and AFU_z, are installed along the line. All the active filter units operate as a harmonic conductance to reduce voltage harmonics. For example, the active filter unit AFU_x performs as given:

$$i_x = G_x \cdot E_{x,h} \tag{1}$$

where $E_{x,h}$ represents the harmonics components of the line voltage E_x. The control of the active filter is implemented in the synchronous reference frame as illustrated in figure 1. The effectiveness of the synchronous reference frame transformation has been proved by various motor drives applications and utility applications[4], [5], [6]. The three-phase line voltages E_{x_a}, E_{x_b}, and E_{x_c} are measured and transformed into $E^e_{x_q}$ and E^e_d in the synchronous reference frame. The ripples of $E^e_{x_q}$ and $E^e_{x_d}$, which represent the line voltage harmonics, are extracted by high-pass filters (HPF). The voltage harmonics $\tilde{E}^e_{x_q}, \tilde{E}^e_{x_d}$ are then multiplied by the conductance command G_x to generate current commands $i^{e*}_{x_q}$, $i^{e*}_{x_d}$ of the active filter. The synchronous reference frame current commands are transformed back to three-phase current commands $i^*_{x_a}$, $i^*_{x_b}$, and $i^*_{x_c}$.

Based on the current commands $i^*_{x_a}$, $i^*_{x_b}$, $i^*_{x_c}$, and the measured currents $i_{x_a}, i_{x_b}, i_{x_c}$, the current regulator calculates the voltage commands $v^*_{x_a}$, $v^*_{x_b}$, $v^*_{x_c}$ as given:

$$\begin{aligned} v^*_{x_a} &= \frac{L_x}{\Delta T}(i^*_{x_a} - i_{x_a}) + E_{x_a} \\ v^*_{x_b} &= \frac{L_x}{\Delta T}(i^*_{x_b} - i_{x_b}) + E_{x_b} \\ v^*_{x_c} &= -1 \cdot (v^*_{x_a} + v^*_{x_b}) \end{aligned} \tag{2}$$

where L_x is the output inductor of the inverter, and ΔT is the sampling period of the digital controller. The Pulse Width Modulator (PWM) then generates the corresponding gating signals so the active filter inverter produces the required

 0-7803-8486-5/04/$20.00

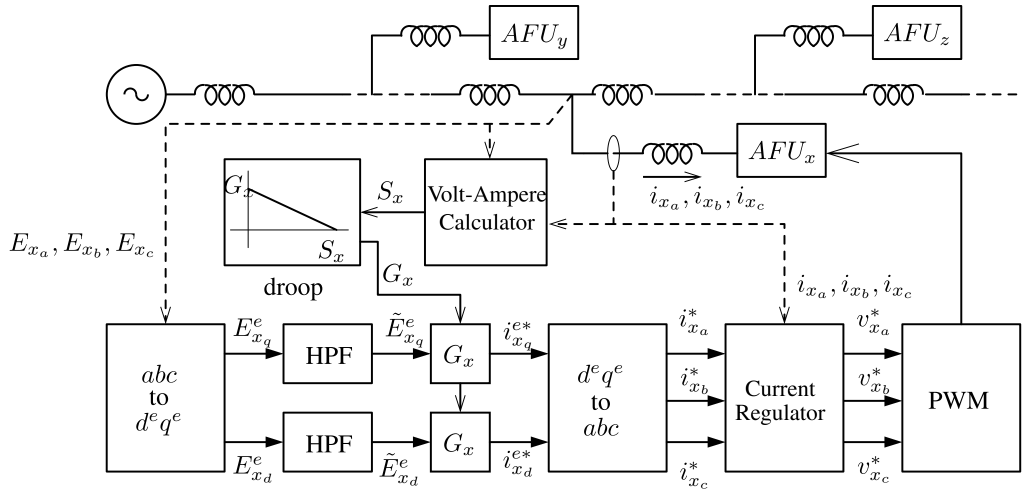

Fig. 1. An active filter unit of the proposed Distributed Active Filter System and the associated control.

voltages. Conventional Sine/Triangle PWM or the space-vector PWM can provide effective tracking of the current commands with high dynamics[7], [8].

In order to share the harmonic filtering workload among the active filter units of the proposed DAFS, a droop relationship between the conductance command and the volt-ampere of the active filter unit is programmed into the controller:

$$\begin{aligned} &G_1 = G_{10} + b_1(S_1 - S_{10}); \quad G_2 = G_{20} + b_2(S_2 - S_{20}); \\ &\cdots\cdots\cdots \quad G_x = G_{x0} + b_x(S_x - S_{x0}); \\ &G_y = G_{y0} + b_y(S_y - S_{y0}); \quad G_z = G_{z0} + b_z(S_z - S_{z0}) \end{aligned} \tag{3}$$

where $G_1, G_2, \cdots, G_x, G_y, G_z$ are the conductance commands for the various active filter units of the proposed DAFS, G_0 and S_0 are the rated operation point of each active filter unit.

The conductance command G_x of AFU_x is determined by the volt-ampere consumption of this active filter unit. To obtain the volt-ampere S_x of AFU_x, the RMS values of voltage and current associated with AFU_x are calculated,

$$\begin{aligned} E_{x_{RMS}} &= \sqrt{\left\{(E^s_{x_q})^2 + (E^s_{x_d})^2\right\}_{dc}} \\ i_{x_{RMS}} &= \sqrt{\left\{(i^s_{x_q})^2 + (i^s_{x_d})^2\right\}_{dc}} \\ S_x &= E_{x_{RMS}} \cdot i_{x_{RMS}} \end{aligned}$$

where the dc values are extracted by low-pass filters. $E^s_{x_q}$ and $E^s_{x_d}$ are the stationary frame values of the line voltages E_{x_a}, E_{x_b} and E_{x_c}, and $i^s_{x_q}$ and $i^s_{x_d}$ are stationary frame values of the current i_{x_a}, i_{x_b} and i_{x_c}.

A simplified circuit given in figure 2 is to demonstrate the effectiveness of $G - S$ droop in distributing harmonic filtering work load. The transmission parameters of section 1 and section 2 of the transmission line are given as follows:

$$\mathbf{T_1} = \begin{bmatrix} \cosh(\gamma_1 l_1) & Z_{c_1}\sinh(\gamma_1 l_1) \\ \frac{1}{Z_{c_1}}\sinh(\gamma_1 l_1) & \cosh(\gamma_1 l_1) \end{bmatrix} \tag{4}$$

$$\mathbf{T_2} = \begin{bmatrix} \cosh(\gamma_2 l_2) & Z_{c_2}\sinh(\gamma_1 l_2) \\ \frac{1}{Z_{c_2}}\sinh(\gamma_2 l_2) & \cosh(\gamma_2 m_2) \end{bmatrix} \tag{5}$$

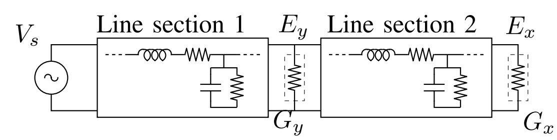

Fig. 2. A simplified circuit for evaluating the effectiveness of the $G - S$ droop.

where γ_1, γ_2 are the propagation constants, Z_{c_1}, Z_{c_2} are the characteristic impedances, and l_1, l_2 are the length of the line sections.

The active filter units are also expressed in the format of transmission parameters for convenience.

$$\mathbf{G_1} = \begin{bmatrix} 1 & 0 \\ G_1 & 1 \end{bmatrix}; \quad \mathbf{G_2} = \begin{bmatrix} 1 & 0 \\ G_2 & 1 \end{bmatrix} \tag{6}$$

Assuming the supply voltage V_s contains harmonics component V_{sh}, the voltage harmonics on bus x and bus y can be calculated as follows:

$$\begin{aligned} E_{x,h} &= V_{sh} \cdot \frac{1}{\begin{bmatrix} 1 & 0 \end{bmatrix} \cdot \mathbf{T_1 G_y T_2 G_x} \begin{bmatrix} 1 \\ 0 \end{bmatrix}} \\ E_{y,h} &= V_{sh} \cdot \frac{\begin{bmatrix} 1 & 0 \end{bmatrix} \mathbf{T_2 G_x} \begin{bmatrix} 1 \\ 0 \end{bmatrix}}{\begin{bmatrix} 1 & 0 \end{bmatrix} \cdot \mathbf{T_1 G_y T_2 G_y} \begin{bmatrix} 1 \\ 0 \end{bmatrix}} \end{aligned} \tag{7}$$

Assuming the active filter units have filtered down the harmonics so significantly that the RMS voltage at these buses is dominated by its fundamental voltage component. Then the volt-ampere associated with AFU_x and AFU_y can be expressed as follows:

$$\begin{aligned} S_x &= 3 \cdot |E_x| \cdot G_x |E_{x,h}| \approx 3|E_{x,f}| \cdot G_x |E_{x,h}| \\ S_y &= 3 \cdot |E_y| \cdot G_y |E_{y,h}| \approx 3|E_{y,f}| \cdot G_y |E_{y,h}| \end{aligned} \tag{8}$$

The droop characteristics of both active filter units are given:

$$G_x = G_{x0} + b_x(S_x - S_{x0}); \quad G_y = G_{y0} + b_y(S_y - S_{y0}) \tag{9}$$

Based on equation (8) and equation (9), the relationship between S_x and b_x can be derived:

$$\begin{aligned} &S_x = 3|E_{x,f}|(G_{x0} + b_x(S_x - S_{x0}))|E_{x,h}| \\ \rightarrow &(1 - 3|E_{x,f}|b_x|E_{x,h}|)S_x = 3|E_{x,f}|(G_{x0} - b_x S_{x0})|E_{x,h}| \\ \rightarrow &S_x \approx \frac{3|E_{x,f}|(G_{x0} - b_x S_{x0})|E_{x,h}|}{3|E_{x,f}|b_x|E_{x,h}|} = \frac{b_x S_{x0} - G_{x0}}{b_x} \end{aligned} \tag{10}$$

Similarly,

$$S_y \approx \frac{3|E_{y,f}|(G_{y0} - b_y S_{y0})|E_{y,h}|}{3|E_{y,f}|b_y|E_{y,h}|} = \frac{b_y S_{y0} - G_{y0}}{b_y} \tag{11}$$

If the droop characteristics of the active filter units are assigned as follows:

$$G_{x0} - b_x S_{x0} = G_{y0} - b_y S_{y0} \tag{12}$$

Then by combining equation (10), equation (11), and equation (12), one can conclude that the volt-ampere of the active filter units will be approximately inversely-proportional to the slope of the droop:

$$b_x S_x \approx b_y S_y \tag{13}$$

Previous derivations show that the slope of the droop should be set in inverse-proportion to the volt-ampere rating of each $AFUs$ to achieve the desired load distribution. This can be extended to the case of multiple installations of active filter units. The slopes of the droops are related to the volt-ampere rating of corresponding active filter units as given,

$$b_1 S_{10} = b_2 S_{20} = \cdots = b_x S_{x0} = b_y S_{y0} = b_z S_{z0} \tag{14}$$

The above droop settings allow harmonic filtering workload being shared in proportion to the volt-ampere rating of the active filter units.

III. Simulation Results

The proposed DAFS is applied a radial power distribution system to demonstrate its capability to share the harmonic filtering workload among the various active filter units with $G - S$ droop characteristics. The circuit model of the radial line is illustrated in figure 4(a) and figure 5(a). This model is used to demonstrate the harmonic amplification effect of long transmission lines [1], [2]. Active filter units of the proposed DAFS and nonlinear loads will be placed at different buses along the line to test the filtering capability. The parameters in the simulation are given as follows:

- Power system: 220 V (line-to-line), 60 Hz. The transmission line parameters are $L_1 = 0.2\,\text{mH}$, $R_1 = 0.05\,\Omega$, $C_1 = 150\,\mu\text{F}$.
- Nonlinear loads: Two diode rectifiers with filter inductor, DC capacitor, and load resistor rated at 2760 VA and 3348 VA are installed at bus 2 and bus 6 of the line respectively.
- Active filters: Two active filter units, AFU_1 and AFU_2 are installed. Both active filter units are implemented by conventional hard-switching three-phase inverters as shown in figure 3. $C = 4500\,\mu\text{F}$, $L = 1.0\,\text{mH}$. The frequency of PWM operation is $f_{pwm} = 10\,\text{kHz}$. The droop parameters are $G_{10} = G_{20} = 0.1\,\Omega^{-1}$, $b_1 = b_2 = -8 \times 10^{-4}\,\text{V}^{-2}$, and $S_{10} = S_{20} = 1.0\,\text{kVA}$.

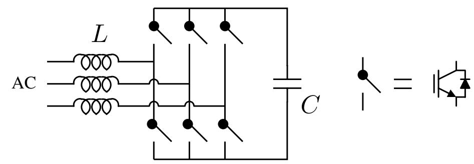

Fig. 3. The inverter of the individual active filter unit.

A. AFU_1 and AFU_2 at Bus 9

The diode-rectifier nonlinear loads are installed at bus 2 and bus 6, and the active filter units AFU_1 and AFU_2 are both at bus 9 as illustrated in figure 4(a). Voltage waveforms on buses 1, 2, 4, 6, and 9 are shown in figure 4 to demonstrate the effectiveness of DAFS. Before the DAFS is started, the harmonic distortion is very severe due to the harmonic amplification along the radial line. Table I shows that the voltage Total Harmonic Distortion (THD) on these buses are significantly reduced as the active filter units start operating. At steady state, AFU_1 and AFU_2 reaches $G_1 = G_2 = 0.46\,\Omega^{-1}$ based on the droop characteristics, and both units absorb 2.02 A (RMS) of harmonic current.

TABLE I
Bus voltage THDs with both AFUs installed at bus 9.

	Bus 1	Bus 2	Bus 4	Bus 6	Bus 9
AFUs off	3.7%	5.9%	7.4%	3.7%	10.2%
AFUs on	2.2%	3.4%	5.6%	4.7%	4.6%

B. AFU_1 at Bus 9 and AFU_2 at Bus 4

In this test, AFU_1 is installed at bus 9, and AFU_2 is installed at bus 4 while the nonlinear diode rectifier loads remain at bus 2 and bus 6 as illustrated in figure 5(a). This arrangement is to test the sharing of harmonic filtering workload and the overall filtering performances of the proposed DAFS. Figure 5 shows the voltage waveforms of various buses.

Figure 5(b) contains the waveforms when both active filter units AFU_1 and AFU_2 operate with $G_1 = G_2 = 0.5\,\Omega^{-1}$. The voltage harmonic distortion is improved as the THDs are reduced by the filtering actions of the AFUs, but the sharing of filtering workload between AFU_1 and AFU_2 is not even. AFU_1 filters 2.78 Arms of harmonic current, while AFU_2 has only 2.40 Arms. The volt-ampere of AFU_1 is 1303 VA, and AFU_2 is 1061 VA, which also indicates un-even share of workload.

Figure 5(c) shows the waveforms when both active filter units operate with droop characteristics. The voltage THDs are improved even further. AFU_1 and AFU_2 filters 2.01 Arms and 2.11 Arms respectively. The active filter units of the DAFS adjust the conductance command G_1 and G_2 based on their own droop characteristics, and result in volt-ampere consumption of 968 VA and 944 VA for AFU_1 and AFU_2, which indicates that the filtering workload is evenly shared between the active filter units of DAFS.

In order to test the dynamic operation of the AFUs, the loading of diode rectifier on Bus 6 increases from 3348 VA to

 0-7803-8486-5/04/$20.00

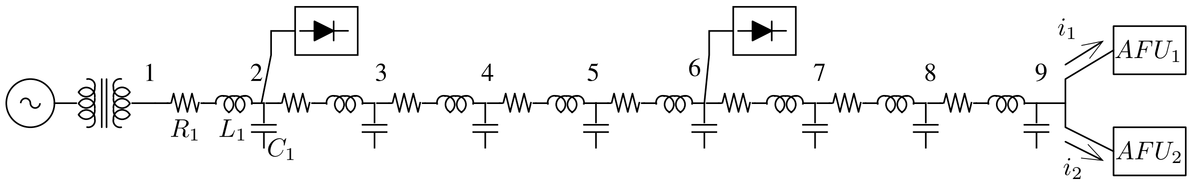

(a) Arrangement of nonlinear loads and DAFS in section III-A.

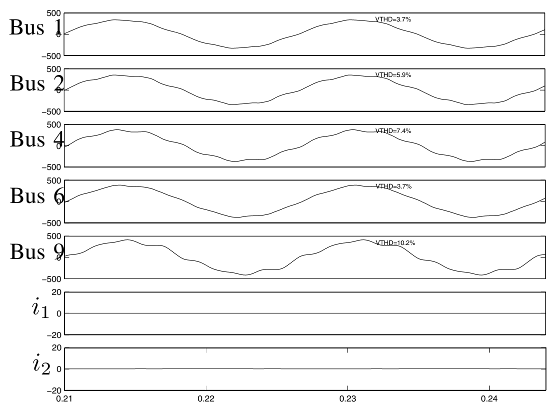

(b) AFUs are off. X axis:sec..

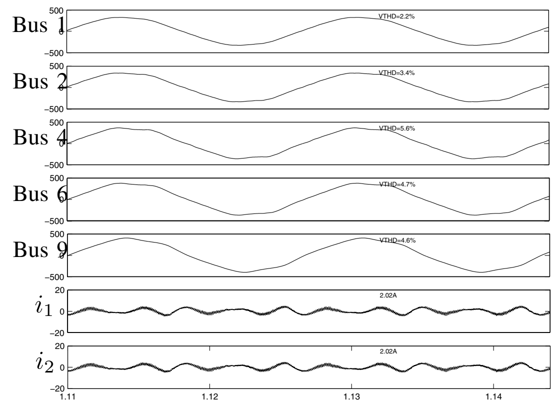

(c) AFU_1 and AFU_2 operate with $G - S$ droop. X axis:sec..

Fig. 4. Simulation results of section III-A: AFUs are installed at the end of the power line; Voltage waveforms at Bus 1, 2, 4, 6, 9, and active filter currents of AFU_1 and AFU_2.

TABLE II
BUS VOLTAGE THDS WITH AFUS INSTALLED AT DIFFERENT LOCATIONS.

	Bus 1	Bus 2	Bus 4	Bus 6	Bus 9
AFUs with constant gain	1.5%	2.3%	3.3%	3.3%	3.5%
AFUs with droop control	1.3%	2.1%	2.8%	2.7%	4.2%

5709 VA at $t = 4\,\mathrm{s}$, and then the loading diode rectifier on Bus 2 increases from 2760 VA to 4758 VA at $t = 7\,\mathrm{s}$. Figure 6(b) shows the volt-ampere associated with the AFUs grows as the voltage harmonics build up along the line due to load increase. And then according to the droop characteristics of the AFUs, the conductance commands G_1 and G_2 will reduce as indicated in figure 6(a). Figure 6(c) shows that the real power of the AFUs rises significantly in response to the load increase.

TABLE III
TRANSITION OF G, S AND P OF AFUS IN RESPONSE TO LOAD INCREASE.

	$t < 4\,\mathrm{sec.}$	$4\,\mathrm{sec.} < t < 7\,\mathrm{sec.}$	$t > 7\,\mathrm{sec.}$
G_1	$0.31\,\Omega^{-1}$	$0.26\,\Omega^{-1}$	$0.19\,\Omega^{-1}$
G_2	$0.52\,\Omega^{-1}$	$0.45\,\Omega^{-1}$	$0.42\,\Omega^{-1}$
S_1	969 VA	974 VA	980 VA
S_2	948 VA	955 VA	958 VA
P_1	40 W	48 W	68 W
P_2	26 W	31 W	34 W

C. AFU_1 and AFU_2 of different VA ratings

Following the circuit arrangement in figure 5(a), the active filter units AFU_1 and AFU_2 are installed on bus 9 and 4 respectively, but their VA ratings are different, and the droop slope of each AFU is inversely proportional to its VA rating as suggested in equation (13). With the $G - S$ droop characteristics, the harmonic filtering workload will be distributed among the AFUs in proportion to their VA rating.

In figure 7(a), AFU_1 is rated at $1.0\,\mathrm{kVA}$, and AFU_2 is rated at $1.5\,\mathrm{kVA}$. As the AFUs reaches steady state, AFU_1 filters 2.02 Arms at 959 VA. AFU_2 filters 3.05 Arms at 1345 VA. The ratio of loading is approximately 1.40 ($AFU_2 : AFU_1$).

In figure 7(b), AFU_1 is rated at $1.5\,\mathrm{kVA}$, and AFU_2 is rated at $1.0\,\mathrm{kVA}$. At steady state, AFU_1 filters 2.97 Arms at 1405 VA, and AFU_2 filters 2.18 Arms at 953 VA. The ratio is approximately 1.47 ($AFU_1 : AFU_2$).

IV. LABORATORY TEST RESULTS

A test bench illustrated in figure 8 is constructed to test the performance of the proposed DAFS. The system parameters are as follows:

- The system voltage is 110 V(line-to-line), 60 Hz. $L = 0.2\,\mathrm{mH}$ and $C = 150\,\mu\mathrm{F}$ are to amply harmonics along the line.
- Nonlinear diode rectifier loads are installed on bus 1 (540 VA) and bus 3(630 VA).

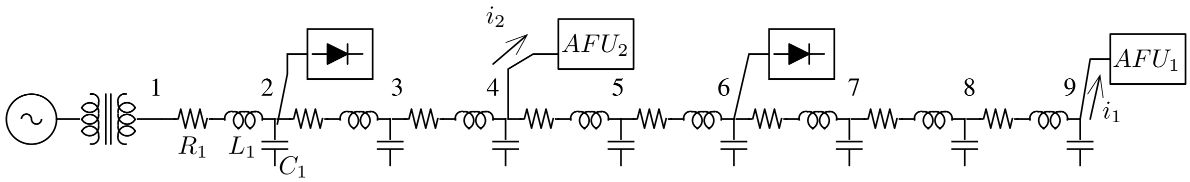

(a) Arrangement of nonlinear loads and DAFS in section III-B.

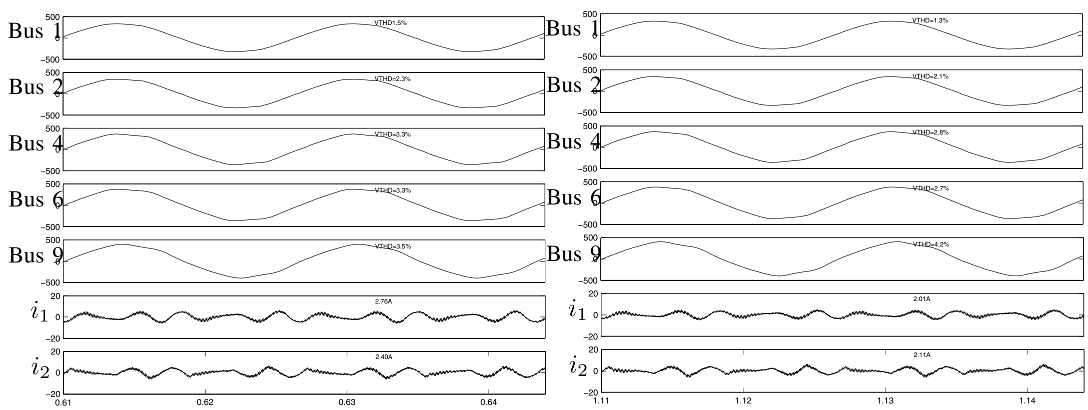

(b) Both AFUs operate with $G_1 = G_2 = 0.5\Omega$.X axis: sec..

(c) AFUs operate with droop characteristics. X axis: sec..

Fig. 5. Simulation results of section III-B: AFUs are installed at different locations; Voltage waveforms at Bus 1, 2, 4, 6, 9, and active filter currents of AFU_1 and AFU_2.

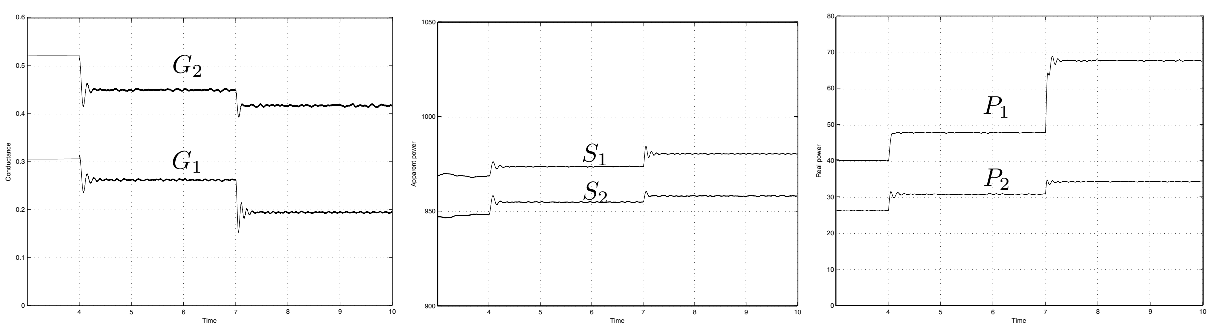

(a) Variation of G_1 and G_2. X axis: sec.; Y axis: Ω^{-1}.

(b) Variation of S_1 and S_2. X axis: sec.; Y axis: VA.

(c) Variation of P_1 and P_2. X axis: sec.; Y axis: Watt.

Fig. 6. Transition of the AFUs operations in response to load increase.

- Active filter units AFU_1 and AFU_2 are installed on bus 4 and bus 2 respectively. The switching frequency of the active filter inverter is 10 kHz.

A. AFU_1 and AFU_2 of the same VA rating

In this test, AFU_1 and AFU_2 are both rated at 150 VA. The slope of the droop is $b_1 = b_2 = -0.02\,\mathrm{V}^{-2}$. Before the active filter units are started, the line voltages on all 4 buses exhibit severe harmonic distortion as shown in figure 9(a). The distortion is significantly reduced as in figure 9(b) after the AFUs start operation. The THDs of line voltages are given in table V. The operation of AFU_1 and AFU_2 are given in figure 10(a) and figure 10(b) respectively. At steady state, AFU_1 absorbs $S_1 \approx 137\,\mathrm{VA}$ with $G_1 \approx 0.29\,\Omega^{-1}$, AFU_2 absorbs $S_2 \approx 139\,\mathrm{VA}$ with $G_2 \approx 0.31\,\Omega^{-1}$. The filtering workload is evenly distributed between AFU_1 and AFU_2 as the test results indicate. Figure 11 shows the conductance command G_1, G_2 and the VA consumption S_1, S_2 of AFU_1 and AFU_2 respectively. AFU_2 is started at t_1, and AFU_1 is engaged at t_2. As both AFUs reach steady state between

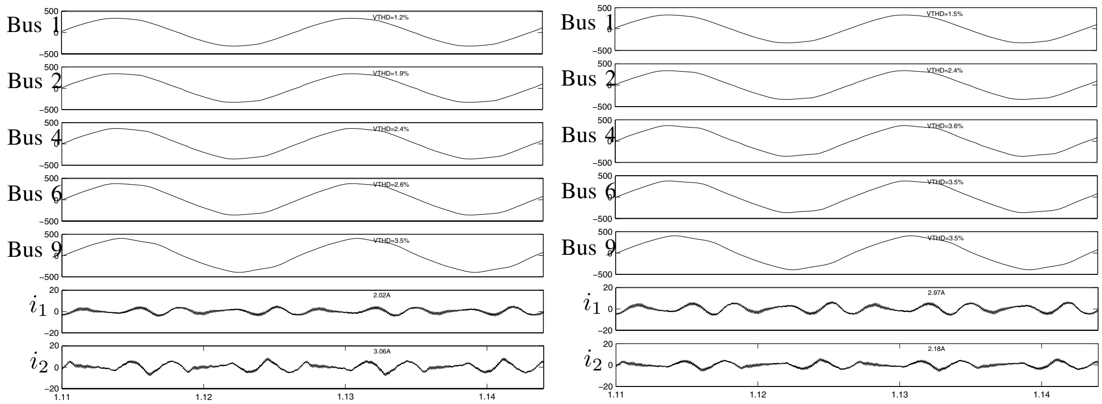

(a) AFU_1 rated at $1kVA$, AFU_2 rated at $1.5kVA$. X axis: sec.

(b) AFU_1 rated at $1.5kVA$, AFU_2 rated at $1.0kVA$. X axis: sec.

Fig. 7. Simulation results of section III-C: AFUs of different VA ratings are installed at different locations; voltage waveforms at Bus 1, 2, 4, 6, 9, and active filter currents of AFU_1 and AFU_2.

TABLE IV
BUS VOLTAGE THDS WITH AFUS OF DIFFERENT RATINGS INSTALLED AT DIFFERENT LOCATIONS.

Bus 1	Bus 2	Bus 4	Bus 6	Bus 9
1.2%	1.9%	2.4%	2.6%	3.5%

(a) AFU_1 rated at 1.0 kVA, AFU_2 rated at 1.5 kVA.

Bus 1	Bus 2	Bus 4	Bus 6	Bus 9
1.5%	2.4%	3.6%	3.5%	3.5%

(b) AFU_1 rated at 1.5 kVA, AFU_2 rated at 1.0 kVA

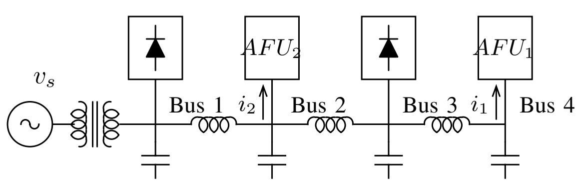

Fig. 8. Laboratory test bench of the proposed DAFS.

t_2 and t_3, $S_1 \approx 138\,\mathrm{VA}$ and $S_2 \approx 140\,\mathrm{VA}$ indicate even distribution of harmonic filtering workload. At t_3, the loading on the rectifier at bus 3 is reduced from 1.63 kVA to 0.3 kVA, and the reduction of harmonics distortion causes S_1 and S_2 of the AFUs to decrease slightly. Then the droop controllers raise the conductance commands G_1 and G_2 respectively as shown in figure 11 and table VI.

B. AFU_1 and AFU_2 of different VA rating

The volt-ampere rating of AFU_1 and AFU_2 are 200 VA and 150 VA respectively in this test. The droop slopes are also adjusted to $b_1 = -0.015\,\mathrm{V}^{-2}$ and $b_2 = -0.02\,\mathrm{V}^{-2}$. As both

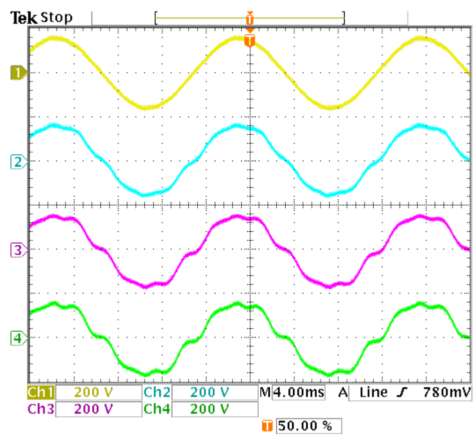

(a) Before the AFUs are started.

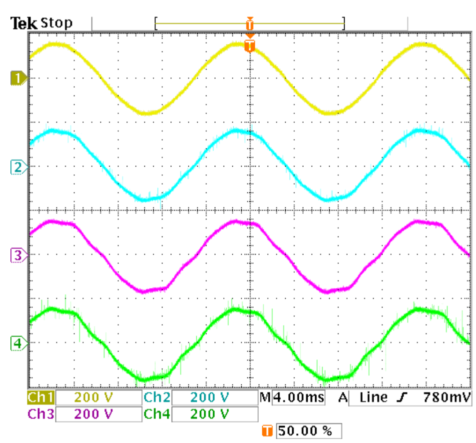

(b) AFUs are in operation.

Fig. 9. Line voltages of all 4 buses. Top to bottom: bus 1, bus 2, bus 3, and bus 4. X axis: 4 ms/div; Y axis: 200 V/div.

TABLE V

THDs OF LINE VOLTAGES.

	Bus 1	Bus 2	Bus 3	Bus 4
AFUs off	1.3%	5.4%	8.5%	9.8%
AFUs on	0.9%	2.2%	3.9%	4.5%

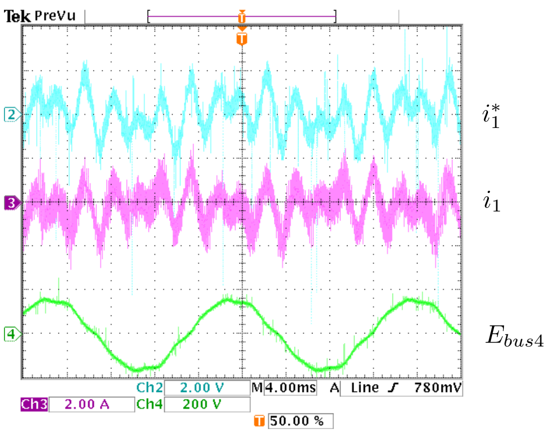

(a) AFU_1

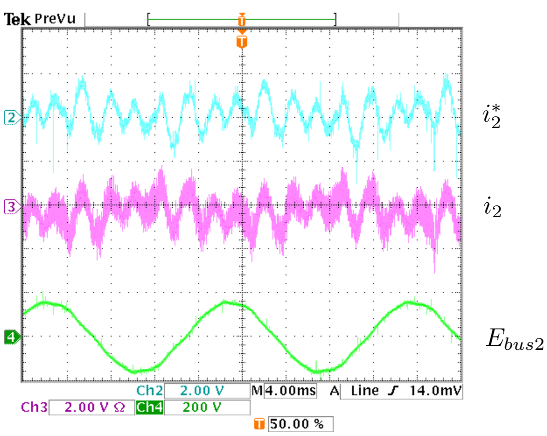

(b) AFU_2

Fig. 10. Operation of the AFU's inverter. Top to bottom: inverter reference current, inverter output current, inverter terminal voltage. X axis: 4 ms/div; Y axis: 2 A/div or 200 V/div.

TABLE VI

OPERATION OF AFUs IN SECTION IV-A.

	$t_1 < t < t_2$	$t < t_2 < t < t_3$	$t > t_3$
G_1	0.152	0.162	0.214
G_2	(off)	0.312	0.372

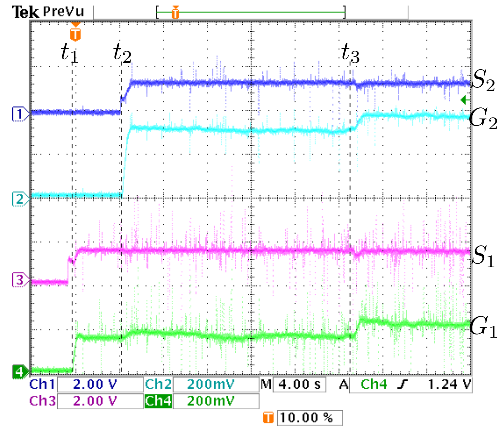

Fig. 11. G_1, S_1 and G_2, S_2 of active filter units. X axis: 4 s/div; Y axis: $0.2\,\Omega^{-1}$/div or 200 VA/div.

AFUs reaches steady state between t_2 and t_3, $S_1 \approx 187$ VA and $S_2 \approx 136$ VA respectively. The AFUs share the filtering workload in approximate proportion to their volt-ampere rating as expected. The same load reduction as in section IV-A is introduced at t_3, S_1 and S_2 reduce slightly and the droop controllers of both units raise the conductance commands G_1 and G_2 in response as shown in figure 12 and table VII.

TABLE VII

OPERATION OF AFUs IN SECTION IV-B.

	$t_1 < t < t_2$	$t < t_2 < t < t_3$	$t > t_3$
G_1	0.24	0.25	0.32
G_2	(off)	0.36	0.40

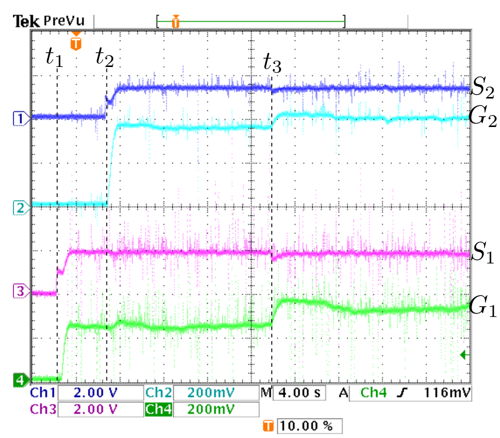

Fig. 12. G_1, S_1 and G_2, S_2 of active filter units. X axis: 4 s/div; Y axis: $0.2\,\Omega^{-1}$/div or 200 VA/div.

V. SUMMARY

A distributed active filter system is proposed in this paper. The conductance-volt ampere $(G - S)$ droop is developed in the proposed DAFS to achieve even distribution of harmonic filtering workload among various active filter units. With proper settings of the droop slope as given in equation (12) and equation (13), each AFU within the DAFS can share the filtering workload based on its own VA capacity. Whether the active filter units are installed at the same location or at different locations, the $G - S$ droop accomplishes the distribution without any communications among AFUs, which is a significant advantage in the deployment of the DAFS.

Computer simulation and laboratory test results validate the effectiveness of the $G - S$ droop characteristics in allocating filtering responsibility. The results also show that a distributed deployment of active filter units can improve voltage THDs along the power lines more effectively than installing active filter at the end of the radial line. Figure 13 shows the THDs of bus voltages along the radial line of the simulation circuit model under different placements of nonlinear loads, and two DAFS deployment configurations, AFU_1, AFU_2 both at bus 9($*$ traces), and AFU_1 at bus 9, AFU_2 at bus 4($\diamond$ traces). If the DAFS is off ($\circ$ traces), the harmonic amplification is severe along the line no matter where the nonlinear loads are as in figure 13. If both AFUs are installed at bus 9, the voltage THD toward the end of line is reduced significantly, but the improvement is not clear in the middle section of the line. With AFU_1 at bus 9 and AFU_2 at bus 4, the voltage THDs along the entire line can be reduced.

The effectiveness of the proposed DAFS on radial transmission lines has been validated by previous simulation and laboratory test results. As the proliferation of power electronics technologies continue to surge, the phenomena of harmonic resonance can occur at the industrial facility. The combination of power factor correction capacitors and the system inductance (power cables, transformers, etc) often result in resonant frequency in the 300-600 Hz range[9]. Most active filter technologies, which focus on compensating harmonic current of nonlinear loads, can not adequately address this issue. The proposed DAFS can deploy several small-rated active filter units at various locations within the facility to damp the harmonic resonance. Compared to a centralized, large-rated active filter, the distributed, small-rated active filters of the DAFS can reduce harmonics in the power system or in a manufacturing facility with improved cost-effectiveness.

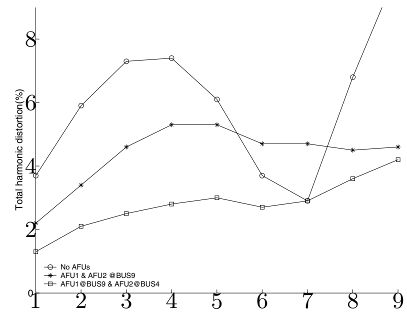

(a) Nonlinear loads at bus 2 and bus 6.

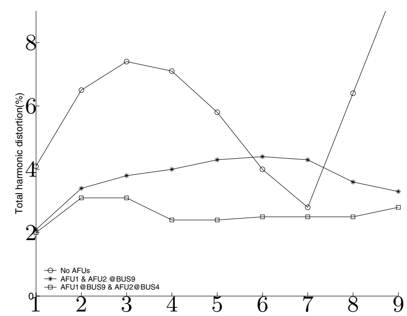

(b) Nonlinear loads at bus 2 and bus 3.

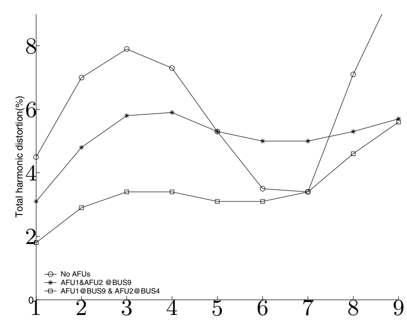

(c) Nonlinear loads at bus 5 and bus 6.

Fig. 13. Voltage THDs under different load and AFUs locations based on simulation.

REFERENCES

[1] K. Wada, H. Fujita, and H. Akagi, "Considerations of a shunt active filter based on voltage detection for installation on a long distribution feeder," *IEEE Transactions on Industry Applications*, pp. 1123–1130, July/August 2002.

[2] P. Jintakosonwit, H. Fujita, H. Akagi, and S. Ogasawara, "Implementation and performance of cooperative control of shunt active filters for harmonic damping throughout a power distribution system," *IEEE Transactions on Industry Applications*, vol. 39, no. 2, pp. 556–564, March/April 2003.

[3] U. Borup, F. Blaabjerg, and P. N. Enjeti, "Sharing of nonlinar load in parallel-connected three-phase converters," *IEEE Transactions on Industry Applications*, vol. 37, no. 6, pp. 1817–1823, November/December 2001.

[4] P. T. Cheng, C. C. Huang, C. C. Pan, and S. Bhattacharya, "Design and implementation of a series voltage sag compensator under practical utility conditions," *IEEE Transactions on Industry Applications*, vol. 39, no. 3, pp. 844–853, May/June 2003.

[5] P. T. Cheng, S. Bhattacharya, and D. Divan, "Experimental verification of dominant harmonic active filter for high power applications," *IEEE Transactions on Industry Applications*, vol. 36, no. 2, pp. 567–577, March/April 2000.

[6] S. Bhattacharya, D. Divan, and B. Banerjee, "Synchronous frame harmonic isolator using active series filter," in *EPE '91 Conference Record*, 1991, pp. 30–35.

[7] T. G. Habetler, "A space vector-based rectifier regulator for ac/dc/ac converters," *IEEE Transactions on Power Electronics*, vol. 8, no. 1, pp. 30–36, January 1993.

[8] R. Wu, S. B. Dewan, and G. R. Slemon, "Analysis of a pwm ac to dc voltage source converter under predicted current control with fixed switching frequency," *IEEE Transactions on Industry Applications*, vol. 27, no. 4, pp. 756–764, July/August 1991.

[9] E. J. Currence, J. E. Plizga, and H. N. Nelson, "Harmonic resonance at a medium-sized industrial plant," *IEEE Transactions on Industry Applications*, vol. 31, no. 3, pp. 682–690, May/June 1995.